

Multiscale computer modeling of nuclear fuel properties at radiation and thermal impacts

S.V.Starikov^{1,2}, A.Yu.Kuksin^{1,2}, D.E.Smirnova^{1,2}, A.V.Lunev¹, V.I.Tseplyaev¹,
M.A.Korneva¹, L.N.Kolotova¹, T.S.Kostyuchenko¹, A.P.Dolgodvorov², P.V.Polovnikov²,
V.D.Ozrin², V.I.Tarasov²

¹*Joint Institute for High Temperatures of RAS, Moscow, Russia*

²*Nuclear Safety Institute of the Russian Academy of Sciences, Moscow, Russia*

E-mail contact of main author: starikov@ihed.ras.ru

Abstract. Multiscale computational approach is used to evaluate microscopic parameters for simulation of UN nuclear fuel behavior at macroscopic models of mechanistic fuel codes. Atomistic simulation of point defects behavior, thermodynamic model for defects density, simulation of primary radiation impact due to collision cascades, calculations of fuel thermodynamic characteristics are presented in this work.

Key Words: nuclear fuel, radiation defects, molecular dynamics, Monte Carlo method.

1. Introduction

Nitride fuel is recognized as one of the most perspective fuels for the liquid metal cooled generation IV fast reactors (FR). The constraint for the design and safety justification of the reactors based on nitride fuel is the poor understanding of its properties especially related to the fuel behavior under irradiation in the reactor core. The extensive experimental studies are performed to eliminate this drawback; however, these investigations are generally rather time-consuming and expensive. Therefore, the approaches based on modern theoretical methods of material science gain a particular importance providing possibility of deeper insight of the processes in the nitride fuels under high temperatures and irradiations.

This approach is especially valuable for tuning of best-estimate codes simulating behavior of the fuel and rods in the reactor core. An example is the new generation mechanistic single rod code BERKUT [1], which is presently under elaboration in IBRAE RAS in the framework of the "New generation codes" branch of the "BREAKTHROUGH" (or "PRORYV") project. The theory based approach allows refining the poorly defined microscopic parameters of specific models implemented into the code. Therefore such calculations are the bridge between the microscale consideration and the meso- or macroscale simulations typical for the mechanistic codes. The calculations are presently used to an increasing extent due to fast development of the computer power and numerical methods for the solution of the atomic-scale problems using quantum mechanics, molecular dynamic (MD) and Monte Carlo methods. Some results of these calculations are given in this work. The concentrations and diffusivities of the point defects were calculated for nitride fuel resulting in important data for analysis of nitride fuel sintering and dissociation [2], [3] as well as for evolution of the fuel microstructure and fission product (FP) behavior [4]–[6]. In addition, the estimates were obtained for the uranium, nitrogen or oxygen self-diffusion coefficients and the microscopic parameters of the FP release from fuel via recoil and knock-out mechanisms.

2. Simulation of fuel defect behavior

Simulation of fuels defects behavior in nitride fuel was carried on by calculations combining density functional theory (DFT) and classical molecular dynamics. DFT calculations pursue the dual goal. On the one hand, they provide completion of the data base for development and validation of the inter-atomic potentials for molecular dynamics. On the other hand, DFT techniques are used for the direct calculations of the defect properties, e.g. their activation energies. At the same time, MD simulations basing on the designed potentials promote finding of important atomic configurations for DFT calculations. Note that the MD-generated atomic configurations obtained by the system energy minimization do not generally correspond to the exact minima and hence should be additionally relaxed by special DFT procedure. Nevertheless, the preliminary MD calculations significantly simplify search of the defect stable states. In this work, the DFT calculations were performed using VASP 5.2 code [7], see details in [8].

2.1. Interatomic potential

To simulate the interatomic interaction in the nitride fuel, the angular-dependent potential (ADP) was designed; details of its development and validation are given in paper [8]. The force-matching method [9] implemented in the potfit code [10] was used for this purpose. In this method the interatomic potential functions are tuned to accurately reproduce the per-atom forces as well as the total energy and stresses computed at the ab initio level for a fine-tuned set of reference structures. Therefore the method allows development of the physically grounded potentials basing on DFT calculations without use of experimental data. The verification shows that the potential reproduces defect energies in agreement with the DFT estimations [8]. In addition, ADP correctly describes the thermodynamic properties.

2.2. MD simulations

The calculations performed with the elaborated potential have shown that the uranium antisite defects (U_N) play an important role in defects behaviour. Uranium atom from the interstitial position (U_i) passes to the nitrogen regular site in the lattice. In this case, formation of U_N occurs with displacing nitrogen atom to the interstitial defect (N_i). Antisite defects are common for compounds formed from the components of similar chemical nature, such as SiC or metallic alloys. In case of uranium mononitride, U_N is quite favourable defect due to relatively small displacements produced in the uranium sub-lattice. Table I shows the basic formation energies of point defects and energy barrier for formation of U_N and N_i from U_i as found from DFT and MD calculations. It is seen that the results of the both approaches are close to each other.

The diffusivity for various point defects (i.e. diffusion coefficients of atoms *via* defect diffusion) was evaluated in this work. The MD calculations were performed for the simulation box containing ca. 2000 atoms and one point defect, see details in [8], [11]. The diffusivity of atoms (U or N) at the presence of given defect is determined by the displacements of all atoms in a system with time:

$$D_{def}^Y = \frac{1}{6t} \sum_{i=1}^M \delta r_i^2, \quad (1)$$

where δr is displacement of the i -th atom, M is the number of atoms of the same type (uranium or nitrogen), t is the computation time; index Y may be equal to U or N and index

def may be equal to I (interstitial) or V (vacancy). The value so calculated is related to the point defect diffusivity as:

$$D_{def}^Y = \alpha D_{def}, \quad (2)$$

where D_{def} is diffusion coefficient of point defect and α is a constant of about 1 (see [12] for details). Unlike the uranium dioxide [12], the diffusivities of atoms in both sub-lattices of UN are quite close to each other. The existence of two regions in the dependence $D_i^U(T)$ was discussed in [8]. The temperature dependencies of calculated diffusivities are shown in FIG. 1.

TABLE I: DEFECT FORMATION ENERGIES AND REACTION ENERGY OF $U_N + N_i$ FORMATION IN eV UNITS

Defect	MD	DFT
Uranium Frenkel pair, E_{FP}^U	6.2	7.1
Nitrogen Frenkel pair, E_{FP}^N	4.0	4.9
Schottky defect, E_{SD}	4.6	4.7
$U_i \rightarrow U_N + N_i$, E_{As}	0.7	0.6

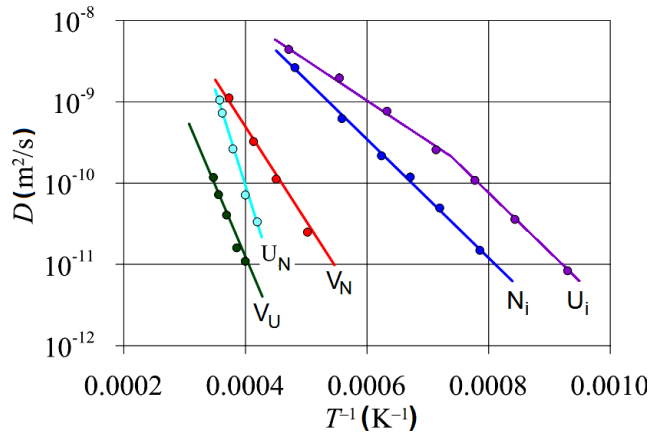


FIG. 1. Nitrogen and Uranium diffusivities via various defects

3. Thermodynamic model of defects concentration

Equations of thermodynamic equilibrium for concentrations of the point defects take the form:

$$\begin{aligned}
 [U_i][V_U] &= \exp(S_{FP}^U / k) \cdot \exp(-E_{FP}^U / kT), \\
 [N_i][V_N] &= \exp(S_{FP}^N / k) \cdot \exp(-E_{FP}^N / kT), \\
 [V_N][V_U] &= \exp(S_{SD} / k) \cdot \exp(-E_{SD} / kT), \\
 \frac{[U_N][N_i]}{[U_i]} &= \exp(S_{As} / k) \cdot \exp(-E_{As} / kT), \\
 x &= [N_i] - [U_i] + [V_U] - [V_N] - 2 \cdot [U_N],
 \end{aligned} \quad (3)$$

where x is the stoichiometry deviation in UN_{1+x} , $[\text{def}]$ is the defect concentration, k is the Boltzmann constant, T is the temperature, S_{def} is the vibration entropy and E_{def} is formation energy of the defect; FP, SD and As denotes the Frenkel pair, Schottky defect and antisite, respectively. The values of S_{def} may be estimated as $6k$ [13]. Dependencies of the defect concentrations on x calculated solving Eq. (3) are shown in *FIG. II* for $T = 1500$ K and $T = 2000$ K.

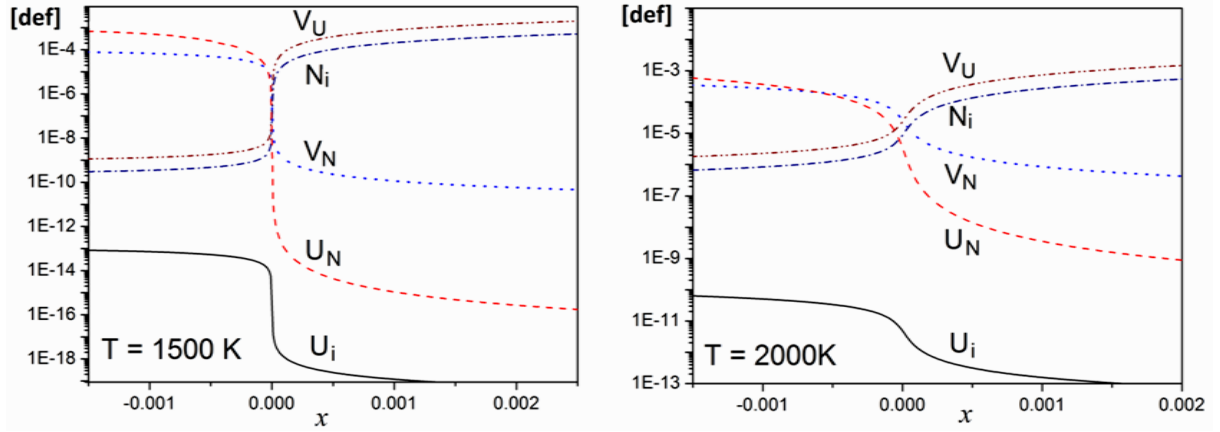


FIG. II. The dependencies of defects concentrations in UN_{1+x} on x (the results are given for two different temperatures).

There is a boundary of physically justified solution for the Eqs. (3). The uranium antisite defects may be considered as nano-size nuclei of pure uranium. At negative value of x , the concentration $[U_N]$ may be about 0.001 that can be interpreted as the formation of uranium. On the other hand, at the positive value of x , large concentrations $[V_U]$ and $[N_i]$ correspond to formation of U_2N_3 . It can be assumed that in case when any defect concentration $[\text{def}]$ achieves value about 10^{-3} , the formation of pure uranium (at negative x) or U_2N_3 (at positive x) takes place. The existence of the narrow area of UN homogeneity agrees well with the experimental data. However, more accurate model should take into account thermodynamic properties of all phases and description of the phase transitions requires further investigation.

For verification of the model, the coefficients of uranium and nitrogen self-diffusion, D^U and D^N were calculated for various temperatures at $x = 0$ by formulas:

$$\begin{aligned} D^U &= [U_i] \cdot D_i^U + [V_U] \cdot D_V^U + [U_N] \cdot D_{As}^U, \\ D^N &= [N_i] \cdot D_i^N + [V_N] \cdot D_V^N + [U_N] \cdot D_{As}^N. \end{aligned} \quad (4)$$

The results of simulation are plotted in *FIG. III*, where the experimental data for the nitrogen [14] and plutonium in PuN [15] self-diffusion coefficients are plotted for the comparison. It is seen the satisfactory agreement of calculations with the experiments, taking into account that the difference between calculated and measured values of D^N may be caused by difference in the conditions. It was supposed $x = 0$ in these calculations, however more correct condition should be related to the nitrogen pressure, which may be estimated using equation:

$$P_{N_2(g)} = A_g [N_i]^2, \quad (5)$$

where A_g is the value depending only on temperature. In this work, the value of A_g was estimated with taking into account the dependencies of uranium and nitrogen self-diffusion coefficients on nitrogen pressure [14,15]. Such procedure allowed us to calculate the dependency of nitrogen pressure on x .

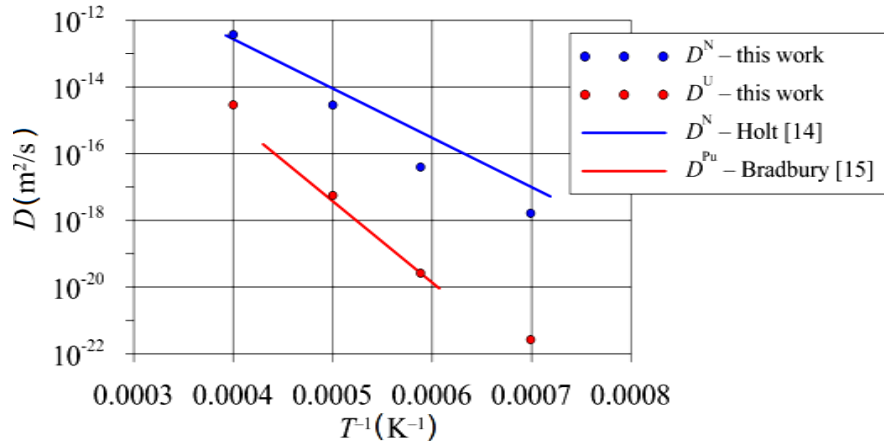


FIG. III. Temperature dependence of nitrogen/uranium self-diffusion coefficients at $x = 0$.

4. Thermodynamic model of nitride fuel

Description of transport properties and chemical behaviour of nitrogen released due to fission requires evaluation of its chemical potential in the fuel matrix. The nitrogen pressure over nonstoichiometric UN calculated by atomistic simulation and the thermodynamic model, Eqs. (3) and (5), is plotted in FIG. IV. Comparison with the available scanty experimental data [16] at $T = 2000$ K demonstrates rather good agreement.

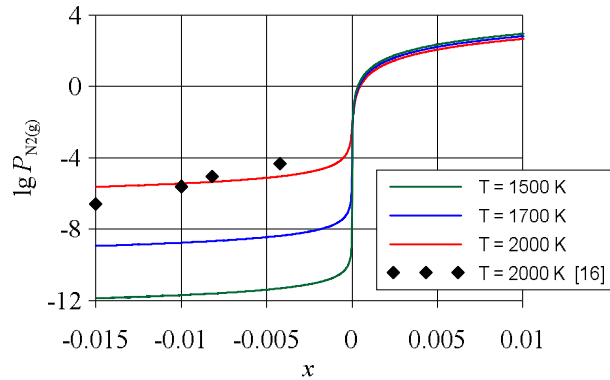


FIG. IV. $N_2(g)$ pressure over UN_{1+x} (in atm units).

For the stoichiometry deviations $x \geq 0$, the nitrogen potential is approximated by correlation:

$$\mu_{N(c)}(x, T) = \frac{1}{2} G_{N_2(g)}^0(T) + \frac{RT}{2} \left(\ln \bar{P}_{N_2}(0, T) + \begin{cases} ax & \text{for } 0 \leq x \leq a^{-1} \\ 1 + \ln ax & \text{for } x > a^{-1} \end{cases} \right), \quad (6)$$

where $G_{N_2(g)}^0$ is the Gibbs energy of the pure matter, T is the temperature, R is universal gas constant, \bar{P}_{N_2} is the nitrogen partial pressure over UN [17] and a is the temperature dependent fitting parameter approximated by function:

$$\log_{10} a = b_0 + b_1 T + b_2 T^2 + b_3 T^3, \quad (7)$$

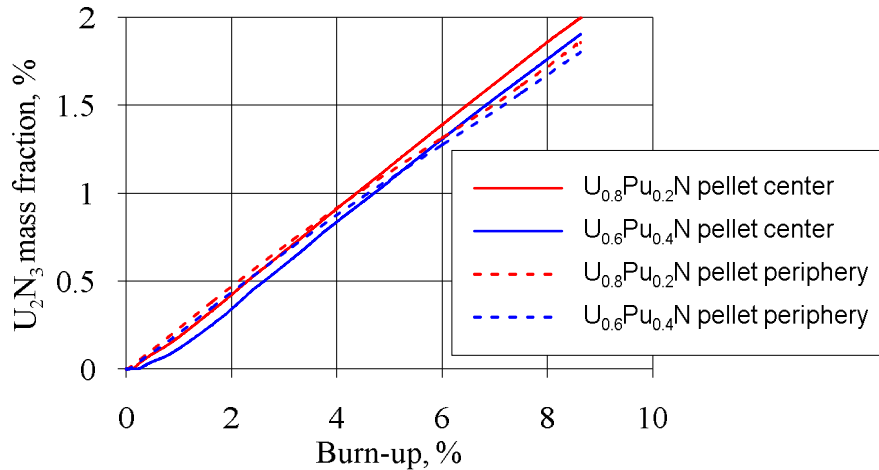
which decreases with the temperature; parameters b_0, b_1, b_2, b_3 are given in Table II.

TABLE II: PARAMETERS OF EQ.(7)

b_0	b_1, K^{-1}	b_2, K^{-2}	b_3, K^{-3}
37.2	-3.81×10^{-2}	1.69×10^{-5}	-2.83×10^{-9}

The testing of the model of nitrogen potential have demonstrated that the calculated results of equilibrium state of the irradiated fuel, in particular its phase composition are in a good agreement obtained by thermodynamic modelling in papers [18], [19].

Equation (6) is included into thermochemical model for the 'U, Pu-FP-N' system implemented into the code BERKUT. Evolution of phase composition of nitride fuels under typical FR irradiation conditions up to burnup $\sim 10\%$ including formation of U_2N_3 phase was simulated by example of two fuel compositions, $U_{0.8}Pu_{0.2}N$ and $U_{0.6}Pu_{0.4}N$. The calculated U_2N_3 mass fractions in the center and peripheral pellet zones are plotted in FIG. V. As seen, the calculations predict decrease of the U_2N_3 content with the increase of the Pu fraction. Moreover the U_2N_3 fraction at the pellet periphery is less than in the center. The reason is the nitrogen binding in the matrix by FPs, mainly Zr and lanthanides, which is more effective at the pellet periphery due to lower temperature resulting in less free nitrogen to form U_2N_3 .

FIG. V. Evolution of U_2N_3 mass fraction.

5. Parameters evaluation of models simulating FP behavior in cascades of secondary knock on atoms

Important characteristic of multiscale model of nuclear fuel behavior is FP diffusivity. Two basic mechanisms are recognized to contribute to the experimentally observed dependence of FP diffusivity on fission rate \dot{F} [20]–[22]: electronic and ballistic stopping of the fission fragments in fuel. The first mechanism is associated with the thermal spike resulted from ionization of the material whereas the second one is associated with the cascades generated by primary knock on atoms (PKA) due to elastic atomic collisions. These mechanisms dominate in oxide fuel at temperatures below $1000^\circ C$, so that the diffusivity is independent on temperature and follows simple correlation $D = A\dot{F}$, where $A \approx 2 \times 10^{-39} m^5 s^{-1}$ [20] for uranium and an order of magnitude less for Xe [21]). Contribution of thermal spike is

suppressed in nitride fuel by an order of magnitude [21] due to higher thermal conductivity in comparison with oxide resulting in increase of the role of the ballistic mechanism.

In this paper the calculations were performed combining Monte Carlo method (binary collision approximation) and MD to evaluate ballistic term of the atomic diffusivities in nitride and oxide fuels. First, the energy distributions of U- and N- or O-PKA were found using computer program SRIM [23] for the set of representative fission fragments (light and heavy ones). The results of calculations are illustrated in FIG.VI by example of PKAs generated in mononitride fuels by ^{138}Xe with the initial energy of 71.4 MeV.

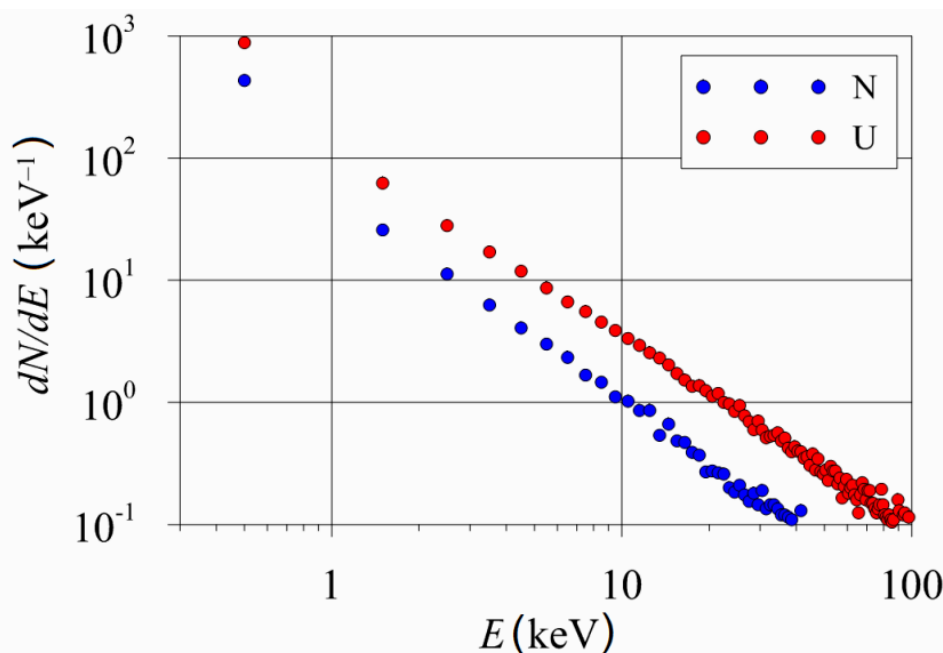


FIG. VI. Energy distribution of PKAs in UN fuel at moving of Xe with initial energy of 71 MeV

The averaged characteristics of the PKA cascades are given in Table III, which demonstrates that the average PKA energies only slightly depend on fuel type. The number of U-PKA is 20% higher in nitride fuel than in oxide one. On the hand, the number of N-PKA is 40% less than that of O-PKA in oxide fuel. Also, the average characteristics are given in the table for the secondary knock-on atoms.

At the second stage, the MD simulations were performed for fuel atoms behavior in the wake of the PKAs with different initial energies. The molecular dynamics code LAMMPS [24] was used for this purpose. For the calculations the 25x25x25 supercell was created. After thermodynamic equilibration (within 6 ps) in the NPT ensemble the velocity directed to the supercell interior was given to PKA. Analysis of the final spatial distributions of the atoms and their convolution with the PKA energy distribution allows evaluation of the mean atom displacements and therefore the a-thermal diffusivities.

The results of calculation are given in Table IV for uranium and oxygen or nitrogen at $\dot{F} = 10^{19} \text{ m}^{-3} \text{ s}^{-1}$. It is seen that uranium a-thermal diffusivity in nitride fuel is 4 times greater than that in oxide fuel. In its turn the latter is three orders of magnitude less than the experimental value. This qualitatively corresponds to the conclusion drawn in [25] that contribution of the ballistic mechanism in oxide fuel do not exceed 1.5% of the total diffusivity.

TABLE III. AVERAGE ENERGIES, NUMBERS AND RANGES OF FISSION FRAGMENTS AND KNOCK-ON ATOMS

Particle	⁹⁵ Sr in UO ₂	⁹⁵ Sr in UN	¹³⁸ Xe in UO ₂	¹³⁸ Xe in UN
Fission fragments				
Energy (MeV)	102	102	71.4	71.4
Range (μm)	8,22	7,15	6,55	5,67
PKA-U				
Energy (keV)	4,21	3,87	6,24	5,91
Number	775	956	888	1103
Range (nm)	3,96	3,84	4,58	4,49
PKA-O or PKA-N				
Energy (keV)	1,60	1,60	2,21	2,01
Number	707	413	869	513
Range (nm)	5,43	5,44	6,71	6,30
ko-U				
Energy (eV)	169	159	175	174
Number	18200	30400	30900	53000
Range (nm)	1,21	1,20	1,24	1,24
ko-O or ko-N				
Energy (eV)	140	140	152	149
Number	62200	50700	106000	87500
Range (nm)	1,11	1,11	1,17	1,15

TABLE IV. A-THERMAL DIFFUSIVITY AT $\dot{F} = 10^{19} \text{ m}^{-3}\text{s}^{-1}$ IN UNITS OF m^2/s .

Atom	UO ₂	UN
U	1.1×10^{-23}	4.5×10^{-23}

The calculations of the ko-atom characteristics can be used to evaluate FP release rate from the fuel near-surface region via ballistic mechanisms. According to Olander [26] the FP fluxes from the unit area of the fuel sample via recoil (Φ^{rec}) and knock-out (Φ^{ko}) mechanisms are calculated as:

$$\Phi^{rec} = \frac{\mu_{ff} y^d \dot{F}}{4}, \quad (8)$$

$$\Phi^{ko}(t) = \frac{1}{\tau^{ko}} \mu_U^{ko} c^\infty(t) \varphi(\lambda \tau^{ko}, t),$$

where μ_{ff} is the fission fragment range, y^d is the FP cumulative yield due to fission, $c^\infty(t)$ is the FP concentration in the fuel bulk, λ is the FP decay constant, $\tau^{ko} = \rho_U / 2n_U^{ko} \dot{F}$ is the typical time of ko-process (ρ_U is the uranium number density), $\varphi(\lambda \tau^{ko}, t)$ is the function satisfying the infinite system of differential equations [26], [27]. The microscopic

parameters, mean ranges μ_U^{ko} , and mean numbers n_U^{ko} , of ko-atoms are appear in Eqs. (8). In early work (e.g. see [28]) these parameters were evaluated analytically using simplifying approaches. The combined Monte Carlo and MD calculations allow refining these estimates. The results of these calculations were implemented into the single rod code BERKUT.

6. Conclusion

Combined calculations based on quantum mechanics, Monte Carlo, molecular dynamics and thermodynamics were performed in this paper for evaluation of concentration and diffusivities of point defects, energy distributions and ranges of PKASs and ko-atoms in oxide and nitride fuels. This allows refining of the microscopic parameters of the model for FP release out of fuel via ballistic mechanisms, contributions of different defects to the atom self-diffusivity in nitride and oxide fuels including a-thermal diffusivity. The results of calculations are implemented in the mechanistic single rod cod BERKUT.

References

- [1] BOLDYREV, A.V., et.al., BERKUT – Best Estimate Code for Modelling of Fast Reactor Fuel Rod Behaviour under Normal and Accidental Conditions, (Proc. Int. Conf. FR-17, Ekaterinburg, 2017), paper 363.
- [2] BARANOV, V.G., et al., “High temperature behaviour of simulated mixed nitrides”, IOP Conference Series: Materials Science and Engineering **130** (2016) 012022.
- [3] LUNEV, A.V., et al., “Kinetic and microstructural studies of thermal decomposition in uranium mononitride compacts subjected to heating in high-purity helium”, J. Nucl. Mater. **475** (2016) 266–273.
- [4] CLAISSE, A., et al., “GGA+U study of uranium mononitride: A comparison of the U-ramping and occupation matrix schemes and incorporation energies of fission products”, J. Nucl. Mater. **478** (2016) 119–124.
- [5] LOPES, D.A., et al., “Ab-initio study of C and O impurities in uranium nitride”, J. Nucl. Mater. **478**(2016) 112–118.
- [6] VESHCHUNOV, M.S., et al., “Development of the advanced mechanistic fuel performance and safety code using the multi-scale approach”, Nucl. Eng. Des. **295** (2015) 116–126.
- [7] KRESSE, G., FURTHMULLER J., “Efficient iterative schemes for *ab initio* total-energy calculations using a plane-wave basis set”, Phys. Rev. B **54** (1996) 11169.
- [8] KUKSIN, A.Y., et al., “The diffusion of point defects in uranium mononitride: Combination of DFT and atomistic simulation with novel potential”, J. Alloy. Comp. **658** (2016) 385–394.
- [9] ERCOLESSI, F., ADAMS, J.B., “Interatomic potential from first-principles calculations: the force-matching method”, Europhys. Lett. **26** (1998) 583–588.
- [10] BROMMER, P., GAHLER, F., “Potfit: effective potentials from *ab initio* data”, Model. Simul. Mater. Sci. Eng. **15** (2007) 295.
- [11] SMIRNOVA, D.E., et al., “Investigation of point defects diffusion in bcc uranium and U-Mo alloys”, J. Nucl. Mater. **458** (2015) 304–311.

- [12] KUKSIN, A.Y., SMIRNOVA, D.E., “Calculation of diffusion coefficients of defects and ions in UO_2 ”, *Physics of the Solid State* **56** (2014) 1214–1223.
- [13] MEHRER, H., *Diffusion in Solids*, Springer, Berlin Heidelberg New York (2007).
- [14] HOLT, J.B., ALMASSY, M.Y., “Nitrogen diffusion in uranium nitride as measured by alpha particle activation of ^{15}N ”, *J. Am. Ceram. Soc.* **52** (1969) 631–635.
- [15] BRADBURY, M.H., MATZKE, H., “Self-diffusion of plutonium in high burn-up simulated (U,Pu)(C,N) and (U,Pu)N”, *J. Nucl. Mater.* **75** (1978) 68–76.
- [16] KHROMOV, YU.F., LYUTIKOV, R.A., “Certain thermodynamic properties of uranium nitride UN_y ”, *Atomic Energy* **49** (1980) 448–452.
- [17] HAYES, S.L., et al., “Material property correlations for uranium mononitride. IV. Thermodynamic properties” *J. Nucl. Mater.* **171** (1990) 300–318.
- [18] LUBIMOV, D.Yu., et al., “Thermodynamic modelling of the phase composition of mixed uranium-plutonium mononitride under fast-neutron irradiation to burn-up 80 GW days/ton and temperature 900–1400 K”, *Atomic Energy*, **114** (2013) 243–248.
- [19] ARAI, Y., et al., “Chemical forms of solid fission products in the irradiated uranium-plutonium mixed nitride fuel”, *J. Nucl. Mater.* **210** (1994) 161–166.
- [20] TURNBULL, J.A., et al., The diffusion coefficients of gaseous and volatile species during the irradiation of uranium dioxide, *J. Nucl. Mater.* **107** (1982) 168–184.
- [21] OLANDER, D., Fission-enhanced diffusion in dispersion fuels, *J. Nucl. Mater.* **372** (2008) 94–105.
- [22] MATZKE, H.J., Radiation enhanced diffusion in UO_2 and $(\text{U,Pu})\text{O}_2$, *Rad. Effects* **75** (1983) 317–325.
- [23] ZIEGLER, J.F., SRIM – The stopping and range of ions in matter (2010). *Nucl. Instrum. Methods Phys. Res. B* **268** (2010) 1818–1823.
- [24] PLIMPTON, S., Fast Parallel Algorithms for Short-Range Molecular Dynamics, *J. Comp. Phys.* **117** (1995) 1–19.
- [25] COOPER, M.W.D., et al., Simulation of radiation driven fission gas diffusion in UO_2 , ThO_2 and PuO_2 , *J. Nucl. Mater.* **481** (2016) 125–133.
- [26] OLANDER, D.R., *Fundamental Aspects of Nuclear Reactor Fuel Elements*, TID-26711-P1 (1976) p. 289–299.
- [27] LEWIS, B.J., Fission product release from nuclear fuel by recoil and knockout, *J. Nucl. Mater.* **148** (1987) 28–42.
- [28] KINCHIN, G. H., PEASE, R. S., The displacement of atoms in solids by radiation. *Progr. Phys.* **18** (1955) 1